EXPERIMENTAL CELL RESEARCH 312 (2006) 2454–2464

available at www.sciencedirect.com

SCIENCE DIRECT®

www.elsevier.com/locate/yexcr

Research Article

# Identification of stem cells from human umbilical cord blood with embryonic and hematopoietic characteristics

*Yong Zhao*, Honglan Wang, Theodore Mazzone*

*Section of Endocrinology, Diabetes and Metabolism, Department of Medicine, University of Illinois at Chicago, 1819 W. Polk Street, Chicago, IL 60612, USA*

ARTICLE INFORMATION

*Article Chronology:*
Received 9 January 2006
Revised version received
4 April 2006
Accepted 15 April 2006
Available online 26 April 2006

*Keywords:*
Stem cell
Umbilical cord blood
Differentiation

ABSTRACT

We identified stem cells from the umbilical cord blood, designated cord blood–stem cells (CB–SC). CB–SC displayed important embryonic stem (ES) cell characteristics including expression of ES-cell-specific molecular markers including transcription factors OCT-4 and Nanog, along with stage-specific embryonic antigen (SSEA)-3 and SSEA-4. CB–SC also expressed hematopoietic cell antigens including CD9, CD45 and CD117, but were negative for CD34. CB–SC displayed very low immunogenicity as indicated by expression of a very low level of major histocompatibility complex (MHC) antigens and failure to stimulate the proliferation of allogeneic lymphocytes. CB–SC could give rise to cells with endothelial-like and neuronal-like characteristics in vitro, as demonstrated by expression of lineage-associated markers. Notably, CB–SC could be stimulated to differentiate into functional insulin-producing cells in vivo and eliminated hyperglycemia after transplantation into a streptozotocin-induced diabetic mouse model. These findings may have significant potential to advance stem-cell-based therapeutics.



## Introduction

The increasing prevalence of chronic human diseases, e.g., cardiovascular disease, diabetes and neuronal degenerative diseases, presents a challenge to find more effective therapies. Stem-cell-based therapy, including embryonic and adult stem cells, provides a rational treatment tool for regenerative medicine and has potential to revolutionize modern therapeutics [1–4]. Because of their high potential for self-renewal and pluripotent differentiation capability, embryonic stem (ES) cells have become a very active area of investigation [1,4,5]. Ethical concerns, however, have limited their availability and practical usefulness [6,7]. Leaving aside these ethical concerns, using in vitro fertilization (IVF) and altered nuclear transfer (ANT) to generate ES cells is made problematic by the complexity of required technologies [7,8]. Recently, human umbilical cord blood has been used as a source of stem cells to repopulate the hematopoietic system and other organs [9–13]. Cord blood provides an abundant source for generation of stem cells, including mesenchymal stem cells [14–16] and monocyte-derived stem cells [17]. Stem cells expressing ES molecular markers have been reported from cord blood after removal of hematopoietic cells (including deletion of all leukocyte common antigen CD45 positive cells) [18]. However, the scarcity of this previously described cell population [18] in cord blood significantly restricts its practical application. In this report, using simple technology, we have identified a novel type of stem cell from umbilical cord blood, designated cord blood–stem cells (CB–SC). We demonstrate that CB–SC share

* *Corresponding author*. Fax: +1 312 413 0437.
E-mail address: yongzhao@uic.edu (Y. Zhao).

0014-4827/$ – see front matter © 2006 Elsevier Inc. All rights reserved.
doi:10.1016/j.yexcr.2006.04.008

properties with human ES cells and hematopoietic cells, including low immunogenicity and differentiation capability.

## Materials and methods

### *Cell culture*

Human umbilical cord blood samples (50–100 ml/unit) were obtained from healthy donors (Life-Source Blood Services, Glenview, IL). Mononuclear cells were isolated using Ficoll-Hypaque ($\gamma$=1.077, Sigma) followed by removing red blood cells using Red Blood Cell Lysis buffer (eBioscience, San Diego, CA). Mononuclear cells were seeded into 8-Well Lab-Tek II Chamber Slides (Fisher Scientific) at 1–2×$10^5$ cells/ml, 0.5 ml/well in RPMI 1640 medium supplemented with 7% fetal bovine serum (Invitrogen, Carlsbad, CA) and incubated at 37°C, 8% $CO_2$ conditions. Cells at 70–80% confluence were passaged every 5–7 days with the fresh RPMI 1640 medium supplemented with 7% fetal bovine serum at ratio 1:2. To expand cells on a large scale, mononuclear cells were initially seeded in 150×15 mm Petri dishes (Becton Dickinson Labware, Franklin Lakes, NJ) at 1×$10^6$ cells/ml, 25 ml/dish in RPMI 1640 medium supplemented with 7% fetal bovine serum. Cells were passaged every 10–14 days at a ratio of 1:2. Because CB–SC tightly adhered to the culture dishes, they were resistant to routine trypsin–EDTA (0.53 mM EDTA) or 5 mM EDTA for detachment. We therefore used incubation in 3.5% lidocaine hydrochloride (Sigma) with 0.5 mM EDTA (diluted from 0.5 M EDTA, pH 8.0, Invitrogen Corporation, Carlsbad, CA) for 5–8 min at room temperature to harvest cells for in vitro analysis and in vivo transplantation.

### *Immunocytochemistry*

Immunostaining was performed as previously described with minor modifications [17]. The cells were incubated for 20 min at room temperature with ImmunoPure Peroxidase Suppressor (Pierce, Rockford, IL) to block endogenous peroxidase activity. For fluorescence-labeled immunostaining, this step was omitted. After incubation with primary antibodies, cells were stained with ABC kit (Vector Laboratories, Burlingame, CA). Immunostaining was performed using the following antibodies: mouse anti-human monoclonal antibodies CD3, CD9, CD11b/Mac-1 (Clone ICRF44), CD20, CD34 (clone 563), R-PE-conjugated mouse anti-human CD34 monoclonal antibody (clone 563), CD45 (HI30), FITC-conjugated mouse anti-human CD45 monoclonal antibody (HI30), CD146 (Clone P1H12), human leukocyte antigen (HLA)-DR, HLA-DQ and isotype-matched antibody $IgG_1\kappa$ were purchased from BD Pharmingen; mouse monoclonal antibodies SSEA-1, SSEA-3, SSEA-4, TRA-1–60, TRA-1–81, Oct-4, Thy-1 (CD90), synaptophysin and tyrosine hydroxylase (TH) were from Chemicon International Inc. (Temecula, CA); mouse monoclonal antibodies CD11b and anti-human von Willebrand factor (vWF) were from Sigma (Saint Louis, MO); microtubule-associated protein (MAP) 1B antibody was from NeoMarkers. Rabbit anti-human polyclonal antibodies: Nanog antibody and glutamate decarboxylase65/67 antibody were from Chemicon; $\gamma$-aminobutyric acid (GABA) antibody was from Sigma; antibodies CD117, Flt-1 (vascular endothelial growth factor receptor 1, VEGF R1) and Flk-1 (VEGF R2) were from NeoMarkers. Rabbit anti-human HLA-ABC polyclonal antibody was from Santa Cruz Biotechnology (Santa Cruz, CA). Mouse monoclonal antibodies to human CD40, CD80 (B7-1) and CD86 (B7-2) were from eBioscience (San Diego, CA). Cells were then incubated with primary antibodies, the mouse $IgG_1\kappa$ (as control for mouse monoclonal antibodies) and normal rabbit IgG (as control for rabbit polyclonal antibodies, Santa Cruz). FITC- or rhodamine (TRITC)-conjugated AffiniPure Donkey anti-mouse IgG antibodies were obtained from Jackson ImmunoResearch Laboratories, INC. (West Grove PA). Alexa Fluor 568-conjugated second antibody was from Molecular Probes (Carlsbad, CA). After staining, the slides were mounted with Mounting Medium (Vector Laboratories, Burlingame, CA). Cells were viewed and photographed using a Zeiss Axiocam Color Camera with Zeiss Axioskop Histology/Digital Fluorescence microscope. The images were acquired with the manufacturer's software and edited using Adobe Photoshop Elements 2.0. When we evaluated cell percentage of expression of cells antigens, we used mouse or rabbit IgG staining as controls for background staining (<1%). Any cellular staining higher than the background staining was regarded as positive staining and then quantified. At least 400 cells were evaluated from five randomly selected fields of each slide.

For double staining assay in the differentiation of endothelial-like cells, both VEGF-treated and untreated cells first completed incorporating acetylated low density lipoprotein labeled with 1,1′-diocatadecyl-3,3,3′,3′-tetramethylindo-carbocyanine perchlorate (Dil-Ac-LDL, Biomedical Technologies Inc., Stroughton, MA) and then were fixed with 4% formaldehyde for 20 min at room temperature and used for immunostaining with specific cell surface marker CD146 as described above.

### *Flow analysis*

For intracellular staining, cells were fixed with 4% paraformaldehyde for 20 min and then permeabilized with 0.5% Triton X-100 (Sigma) for 5–6 min at room temperature. For cell surface staining, the fixation and permeabilization steps were omitted. Cells were incubated with 2.5% horse serum (Vector Laboratories) at room temperature to block non-specific staining. Cells were incubated with primary antibodies for 45 min at 4°C and then washed with cold PBS. Cells were stained with FITC-conjugated second antibodies for another 45 min at 4°C and followed by flow analysis. Isotype-matched mouse $IgG_1\kappa$ antibody or normal rabbit IgG served as negative controls. After staining, cells were analyzed using a Beckman-Coulter Elite ESP.

### *Mixed lymphocyte reaction (MLR)*

CB–SC as stimulator were seeded in 8-Well Lab-Tek II Chamber Slides at 1×$10^5$ cells/ml, 0.5 ml/well in RPMI 1640 medium supplemented with 7% fetal bovine serum and

incubated at 37°C, 8% $CO_2$ conditions overnight. Allogenetic lymphocytes as responder were collected from buffy coats of healthy donors (Life-Source Blood Services, Glenview, IL) after removing all attached cells and then cocultured with CB–SC in triplicate at increasing CB–SC:lymphocyte ratios (1:10, 1:20 and 1:40). Lymphocyte cultures without CB–SC served as controls. After 6 days, the suspended lymphocytes were collected and counted.

### *Cell differentiation*

We used CB–SC cultured for 1–2 months for experiments examining cell differentiation. For differentiation to endothelial-like cells, CB–SC were treated with 50 ng/ml VEGF (R&D System, Minneapolis, MN) in RPMI 1640 medium supplemented with 7% fetal bovine serum and incubated at 37°C, 8% $CO_2$. After 10–14 days, VEGF-treated and -untreated CB–SC were examined for endothelial-associated markers. For differentiation to neuronal-like cells, CB–SC at 70% confluence were treated with 100 ng/ml nerve growth factor (NGF, R&D System) in RPMI 1640 medium supplemented with 7% fetal bovine serum in 8-well Lab-Tek chamber slides (Nunc, Naperville, IL) and incubated at 37°C, 8% $CO_2$. After 10–14 days, NGF-treated and -untreated CB–SC were examined with neuronal markers.

### *Transplantation of CB–SC into diabetic mice*

Diabetes in Balb/c nude male mice was induced with a single intraperitoneal injection of streptozotocin (STZ) (Sigma) 220 mg/kg of body weight, freshly dissolved in citrate buffer (pH 4.5). Blood glucose levels were evaluated daily between 9 and 11 A.M. under nonfasting conditions. Diabetes was confirmed by the presence of weight loss, polyuria and nonfasting blood glucose levels >350 mg/dl for 2 consecutive days. Diabetic mice were used for transplantation according to a protocol approved by the Animal Care Committee (ACC) of University of Illinois at Chicago. In brief, CB–SC at dosage of 5 million cells/mouse in 0.5 ml physiological saline were injected into the peritoneal cavity by injection with 27-gauge needle, normally on day 3 following the injection of streptozotocin. The control mice were injected only with an equal volume of physiological saline. Blood glucose levels were monitored using an AccuChek glucose detector (Roche Diagnostics, Indianapolis, IN).

Seven days after transplantation, we performed intraperitoneal glucose tolerance testing (IPGTT). Mice (CB–SC-transplanted diabetic mice, untransplanted diabetic mice and non-diabetic mice) were fasted overnight (12 h). Mice were weighed and injected intraperitoneally with a bolus of glucose (2 mg/g of body weight). Blood was then drawn from a tail vein at 0, 5, 10, 20, 30, 45, 60, 90 and 120 min after glucose administration. Glucose levels were measured from whole tail vein blood as described above. To measure human C-peptide, blood samples were collected from the tail vein during a 20-min time period before and following IPGTT. Blood human C-peptide level was detected by using an ultrasensitive human C-peptide enzyme-linked immunosorbent assay (ELISA) kit (Alpco Diagnostics, Windham, NH) following the manufacturer's protocols. This assay does not detect mouse C-peptide.

### *Statistics*

Statistical analyses of data were performed by the paired Student's *t* test to determine statistical significance. Values are given as mean ± SD (standard deviation).

## Results

### *CB–SC display embryonic and hematopoietic markers*

We cultured mononuclear cells of cord blood in 8-well Lab-Tek chamber slides and observed that the attached cell population (approximately 5% of mononuclear cells) could proliferate. These cells were therefore passaged every 5–7 days, up to a total of 7 passages over 2 months. Based on a growth curve generated over 12 days (Fig. 1A), we estimated the doubling time of CB–SC to be 2.8 days. Cell proliferation ability decreased in the longer-term cultures (over 3 months). To characterize these cells, we initially evaluated expression of embryonic [19–21] and hematopoietic stem cell markers [22]. Immunostaining CB–SC on day 1 after isolation demonstrated the presence of hematopoietic cell antigens including tetraspanin CD9, leukocyte common antigen CD45 and stem cell factor receptor CD117 (Fig. 1B). These cells did not express the macrophage marker CD11b/Mac-1, T lymphocyte marker CD3, B lymphocyte marker CD20 or the hematopoietic stem cell marker CD34 (Fig. 1B). These results suggest that CB–SC are phenotypically distinct from macrophages,

**Fig. 1 – Characterization of CB–SC for embryonic and hematopoietic cell markers. (A) Quantitation of attached cells per well over 12 days. Freshly isolated mononuclear cells were planted on day 1 in 8-Well Lab-Tek II chamber slides. (B) Cells stained with antibodies to leukocyte common antigen CD45 (green) and other hematopoietic cell markers (red), along with DAPI staining (blue). Mononuclear cells were cultured in 8-well Lab-Tek chamber slides overnight and then fixed for immunostaining. We used an FITC-conjugated antibody for CD45, Alexa Fluor 568-conjugated second antibody for CD117 and rhodamine (TRITC)-conjugated second antibody for other primary antibodies. Mouse IgG served as negative control for mouse monoclonal antibodies CD3, CD9, CD11b/Mac-1, CD20 and CD34. Rabbit IgG served as negative control for rabbit polyclonal CD117 antibody. Cells were photographed using Zeiss LSM 510 META confocal microscope. Scale bar, 5 μm. (C) Expression of ES cell markers on 15-day CB–SC. Normal rabbit IgG served as negative for Nanog polyclonal antibody; mouse IgG antibody served as negative control for other monoclonal antibodies. Scale bar, 57 μm. (D) Expression of hematopoietic cell markers on 15-day CB–SC. Normal rabbit IgG served as negative control for CD117 polyclonal antibody; mouse IgG antibody served as negative control for other monoclonal antibodies. Scale bar, 47 μm. Data represent one of at least five experiments with similar results.**

lymphocytes and previously characterized CD34+ hematopoietic stem cells. To further characterize these cells, we evaluated expression of embryonic markers. Immunostaining results showed strong expression of ES-cell-specific markers, including two critical transcription factors Oct-4 and Nanog (related to self-renewal and pluripotentiality of ES cells [21]), along with stage-specific embryonic antigen (SSEA)-3 and SSEA-4 [20]. These cells also showed weak expression of tumor rejection antigen (TRA)-1–60 and TRA-1–81 and no expression of SSEA-1 (Fig. 1C). Consistent with staining results at the early stage (Fig. 1B), all cells strongly expressed hematopoietic cell markers, including CD9, CD45 and CD117, but remained negative for CD3, CD11b/Mac-1, CD20, CD34 and CD90/Thy-1 surface antigens (Fig. 1D). Notably, flow analysis demonstrated that CB–SC maintained in 7% FBS–RPMI 1640 medium retained these phenotypes for over 2 months (Figs. 2A and B). The above results were obtained from 8 cord blood units yielding similar results, including fresh and liquid-nitrogen-frozen preparations. Based on our current studies, CB–SC can be generated from

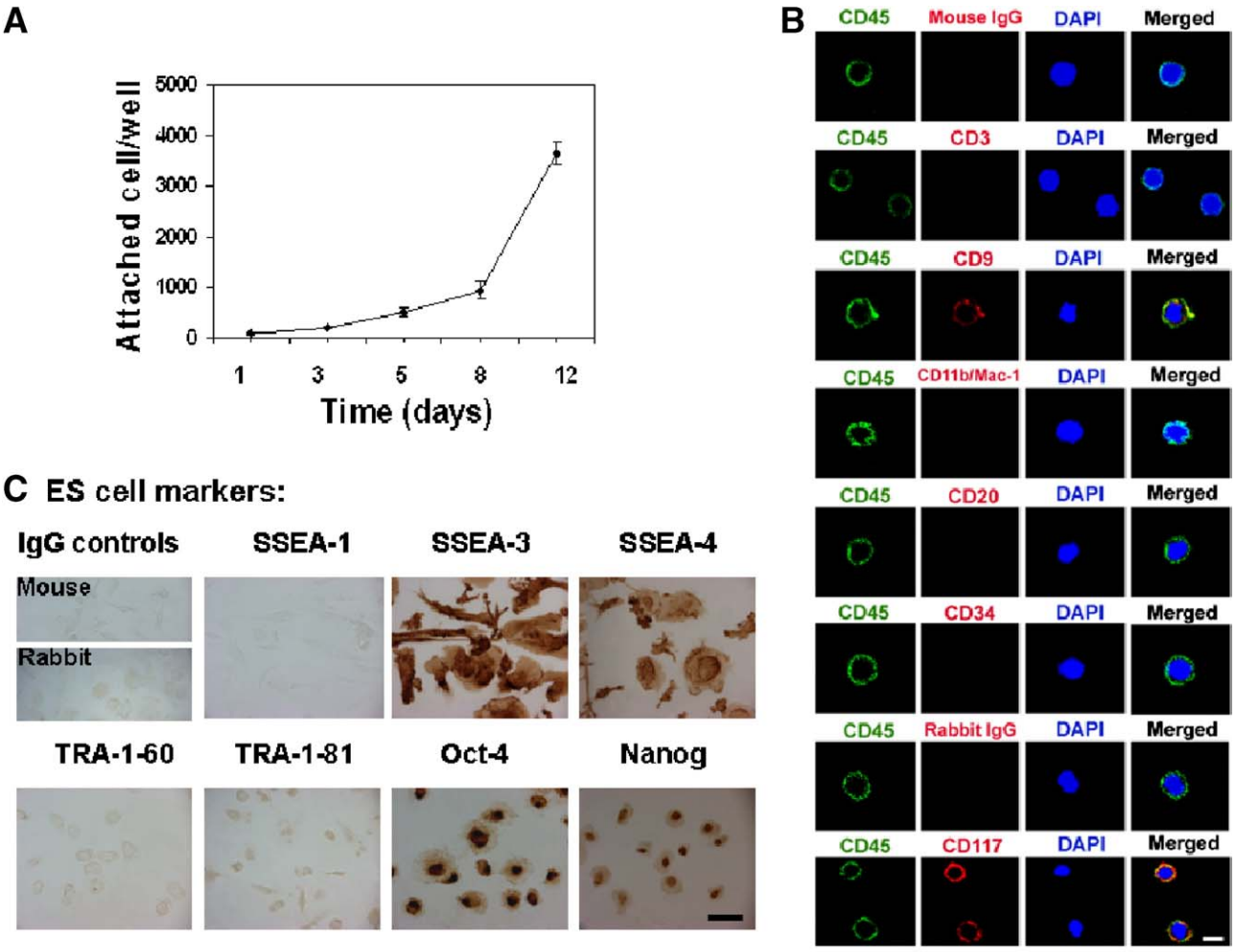

every cord blood unit. Together, these data indicate that CB–SC represent a unique cell population displaying both embryonic and hematopoietic cell characteristics.

### *Evaluation of the immunogenicity-associated phenotype of CB–SC*

A major concern using stem cells for therapeutics is their immunogenicity, leading to immune rejection. Cellular immunogenicity is mainly determined by the major histocompatibility complex (MHC) including MHC class I molecule (HLA-ABC) and MHC class II molecules (HLA-DR and HLA-DQ) [23]. To more fully characterize CB-SC, we evaluated CB–SC for immunogenicity-associated phenotypes including HLA-ABC, HLA-DR and HLA-DQ, along with immune response-related costimulating molecules CD40, CD80, and CD86. Immunostaining for two critical MHC molecules demonstrated that only 5% of cells expressed HLA-ABC, and HLA-DR was completely negative (Fig. 3A). These levels of expression are similar to levels of expression reported in human ES cells [23]. Approximately 6% of cells showed weak expression for CD40 and CD80; ≈30% of cells expressed HLA-DQ; ≈22% of cells expressed CD86 (Fig. 3A). To more fully evaluate their immunogenicity, we performed a functional analysis using the mixed lymphocyte reaction. As shown in Fig.

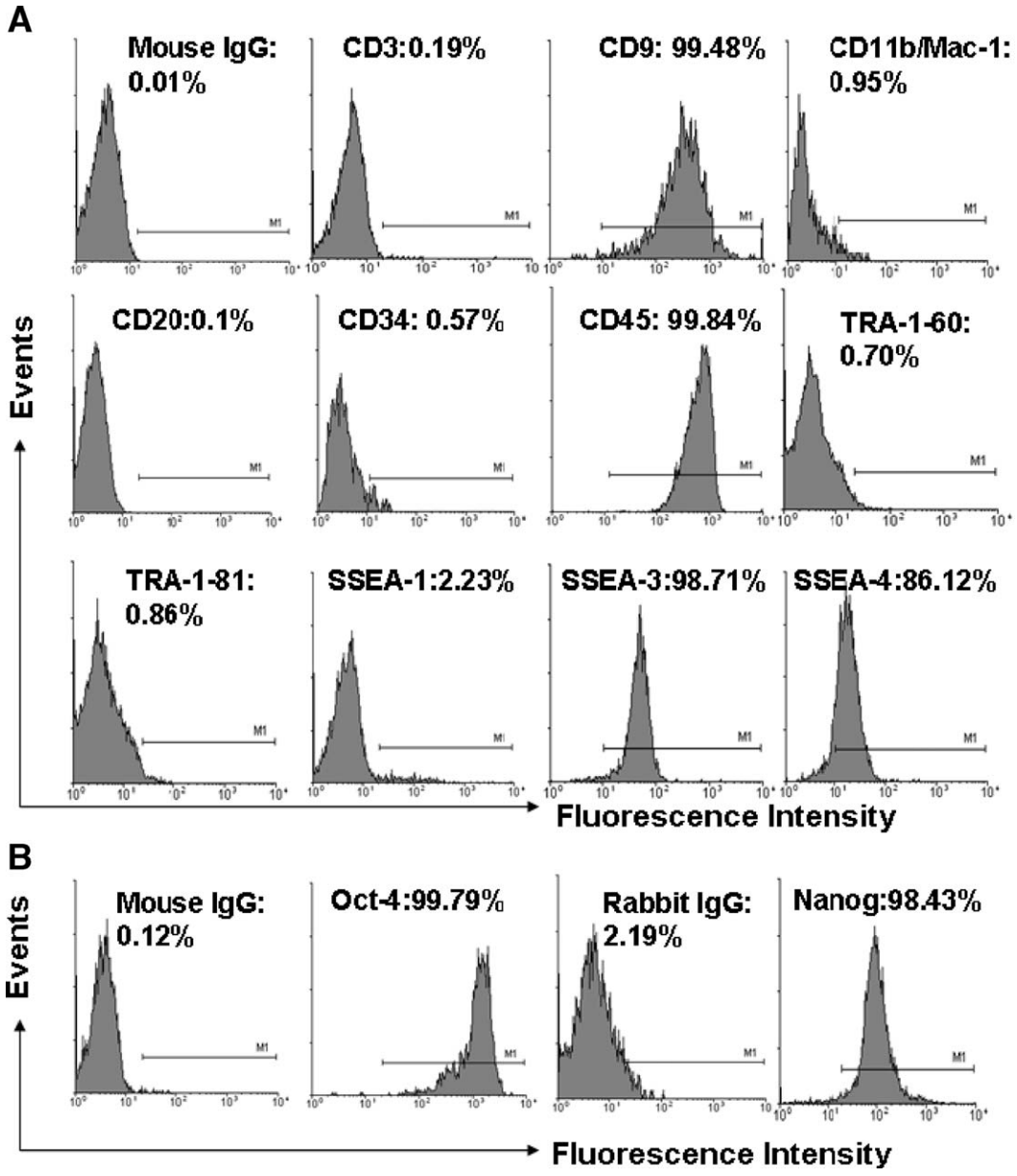


**Fig. 2 – Flow analyses of embryonic and hematopoietic cell markers on CB–SC. Cells were cultured with regular culture medium in Petri dishes for 2 months and then harvested for flow analyses on cell surface antigens (A) and transcription factors (B). Normal rabbit IgG served as negative for Nanog polyclonal antibody; mouse IgG antibody served as negative control for other monoclonal antibodies. Data represent results from three experiments with the similar results.**

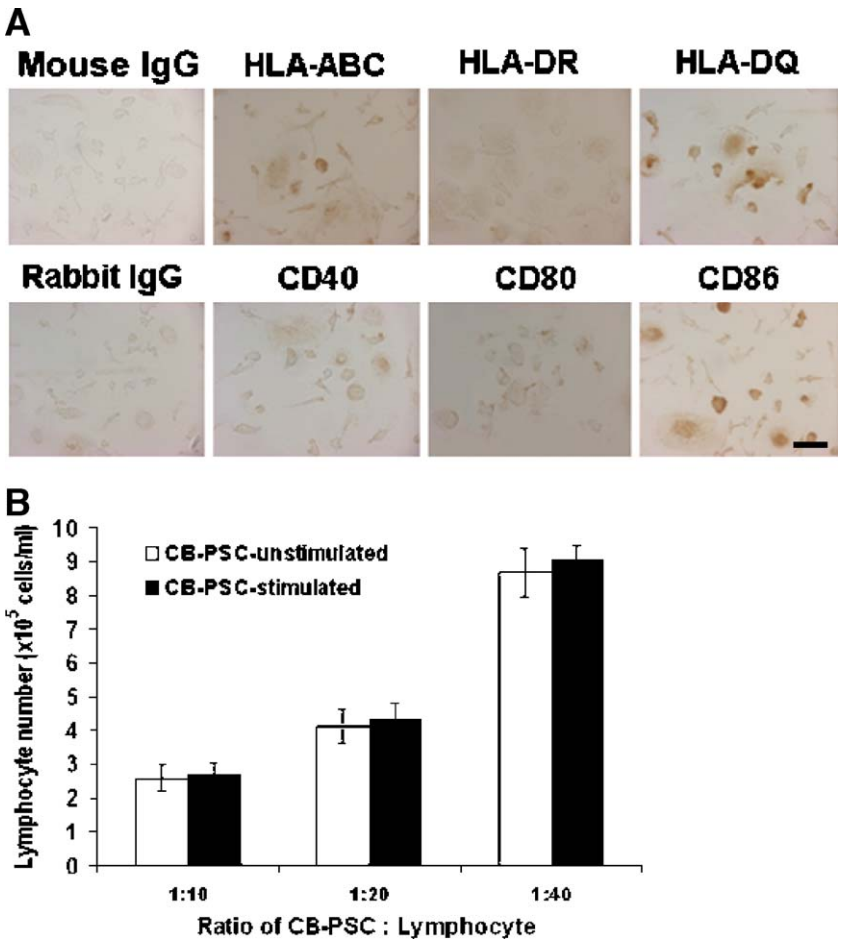


**Fig. 3 – Evaluation of the immunogenicity of CB–SC. (A) Examination of immune-associated markers on CB–SC. Immunostaining results were obtained from four cord blood preparations and yielded the similar results. Normal rabbit IgG served as negative for HLA-ABC polyclonal antibody; isotype-matched mouse IgG antibody served as negative control for other monoclonal antibodies. Scale bar, 47 μm. (B) Mixed lymphocyte reaction (MLR). CB–SC were cocultured with allogeneic lymphocytes from human peripheral blood for 6 days at different ratios. Cell number represents mean (±SD) of three experiments.**

3B, CB–SC did not stimulate lymphocyte proliferation in an allogeneic mixed lymphocyte reaction, consistent with low immunogenicity demonstrated by immunostaining.

### *Differentiation of CB–SC into endothelial-like cells*

To evaluate the differentiation potential of CB–SC, we examined differentiation to endothelial-like cells. CB–SC were treated with vascular endothelial growth factor (VEGF, 50 ng/ml [17,22]) for 10–14 days. Immunostaining results showed that ≈97% of VEGF-treated CB–SC expressed endothelial cell markers, including Flt-1 (VEGF receptor 1), Flk-1 (VEGF receptor 2) and von Willebrand Factor (vWF), and 76% of cells were positive for transmembrane glycoprotein CD146 (Fig. 4A, bottom of left panel). Untreated CB–SC did not express these antigens (Fig. 4A, top of left panel). Hematopoietic antigens including CD45 and CD117 were down-regulated in VEGF-treated cells (Fig. 4A, right panel). In vitro functional analysis showed that both the VEGF-treated and untreated CB–SC possessed strong ability to incorporate acetylated low density lipoprotein (Ac-LDL) (Fig. 4A). Additionally, the cellular morphology of VEGF-treated CB–SC changed to broad endothelial-like cells with spontaneous formation of chain-like structures (Fig. 4B). We further characterized these structures with specific endothelial cell marker CD146 and endocytosis of Ac-LDL and showed that they were double positive (Fig. 4C).

### *Differentiation of CB–SC into neuronal-like cells*

The above experiments demonstrate that CB–SC produced endothelial-like cells, which arise from embryonic mesoderm [4,24]. We next evaluated the potential of CB–SC to differentiate to ectoderm-derived neuronal cells [4,25]. CB–SC were treated with neuronal growth factor (NGF, 200 ng/ml [22]) for 10–14 days. Following this treatment, CB–SC displayed elongated and/or branched morphologies and formed neuronal-like networks through elongated cell processes (Fig. 5C). Immunostaining demonstrated that they were positive for neuronal marker microtubule-associated protein 1B (Fig. 5C); untreated cells were negative or showed background staining (Fig. 5A). To further evaluate neuronal phenotypes, we examined NGF-treated cells for

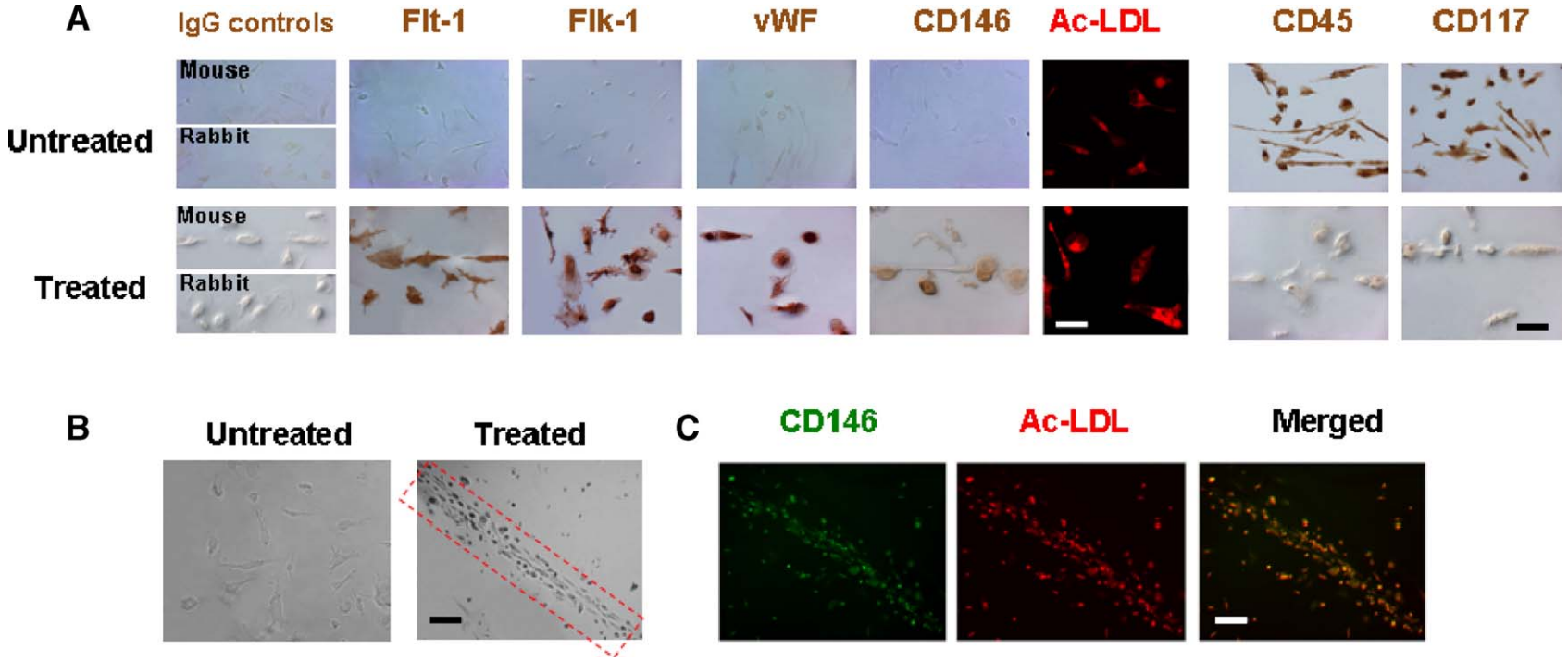


**Fig. 4 – Differentiation of CB–SC into endothelial-like cells. CB–SC were treated with 50 ng/ml VEGF for 10–14 days and then prepared for immunostaining. Untreated cells served as control. (A) VEGF-treated or untreated CB–SC were stained with endothelial cell markers Flt-1, Flk-1, von Willebrand Factor (vWF) and CD146 (left panel); also evaluated with hematopoietic cell markers CD45 and CD117 (right panel). Scale bar, 60 μm. (B) Phase contrast image showed formation of cell chain-like structure in VEGF-treated CB–SC. Untreated cells served as control. Scale bar, 50 μm. (C) Cells in chain-like structure were double stained with the acetylated low density lipoprotein (Ac-LDL) (red) and CD146 (green) and then merged (yellow). The merged image showed overlap of CD146 and Ac-LDL staining. Cells were photographed with a MicroMAX 5 MHz Digital Camera using Zeiss Axiovert 100TV Fluorescence microscope. Scale bar, 50 μm. The images are representative of five experiments.**

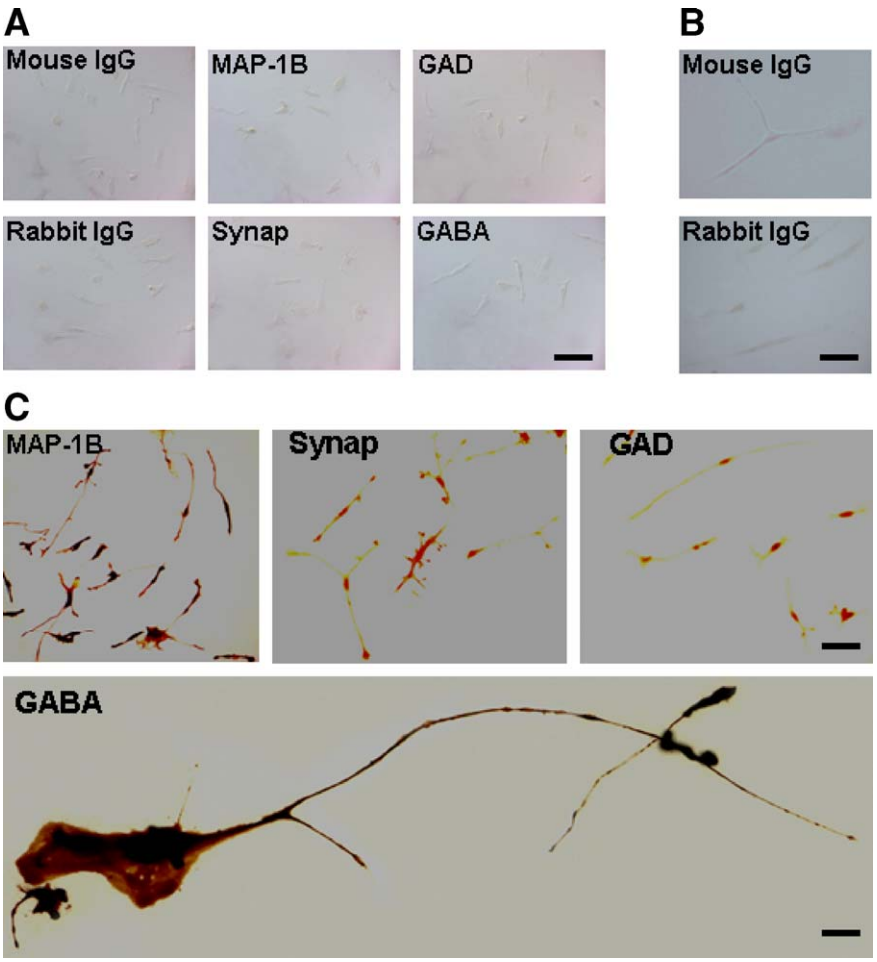


**Fig. 5 – Differentiation of CB–SC into neuronal-like cells. CB–SC were treated with 200 ng/ml NGF for 10–14 days and then prepared for immunostaining. Untreated cells served as control. (A) NGF-untreated cells were stained with neuronal markers. Scale bar, 57 μm. (B and C) showed NGF-treated cells. (B) Mouse IgG served as negative control for microtubule-associated protein 1B (MAP-1b) and synaptophysin (Synap); rabbit IgG served as negative control for γ-aminobutyric acid (GABA) and glutamate decarboxylase65/67 (GAD). Scale bar, 57 μm. (C) Expression of neuronal-cell-specific markers on NGF-treated cells. Scale bar is 37 μm. The images are representative of three experiments.**

neuronal function-associated markers [26]. As shown in Fig. 5C, 85% of cells were positive for synaptophysin; 78% of cells expressed neuronal transmitter γ-aminobutyric acid (GABA) along with its critical synthesizing enzyme glutamic acid decarboxylase (GAD). Untreated CB–SC cells were negative for these markers (Fig. 5A). Less than 5% of NGF-treated cells expressed dopaminergic neuron-associated tyrosine hydroxylase (TH) (data not shown). Hematopoietic antigens including CD9, CD45 and CD117 were down-regulated following treatment with NGF (data not shown). Results suggest that NGF-treated CB–SC can give rise to GABAergic-like neurons.

### *In vivo differentiation of CB–SC into functional insulin-producing cells*

The above results have shown that CB–SC can differentiate into mesoderm-derived endothelial-like cells, along with ectoderm-derived neuronal-like cells in vitro. To provide additional evidence of CB–SC's differentiation potential, we investigated whether CB–SC can differentiate into endoderm-derived insulin-producing cells [2,4] in vivo. Because we transplanted human stem cells, the immune-deficient mice must be used to avoid immune rejection. To date, there is not an ideal type 1 diabetic model (caused by autoimmune destruction) available for xenograft transplantation. We therefore performed in vivo transplantation of CB–SC into streptozotocin (STZ)-induced diabetic Balb/c nude mice and evaluated their capacity to correct hyperglycemia. CB–SC were injected into the peritoneal cavity of the diabetic mice. STZ-induced diabetic mice received physiological saline without cellular implantation as a control. CB–SC-transplanted mice displayed significantly lower blood glucose levels (Fig. 6A). Furthermore, intraperitoneal glucose tolerance testing (IPGTT) demonstrated physiological responses of transplanted CB–SC cells. Blood glucose of normal non-diabetic mice peaked between 5 and 10 min and returned to normal level 30 min following glucose challenge. Blood glucose of CB–SC-transplanted diabetic mice peaked at 20 min followed by a return to

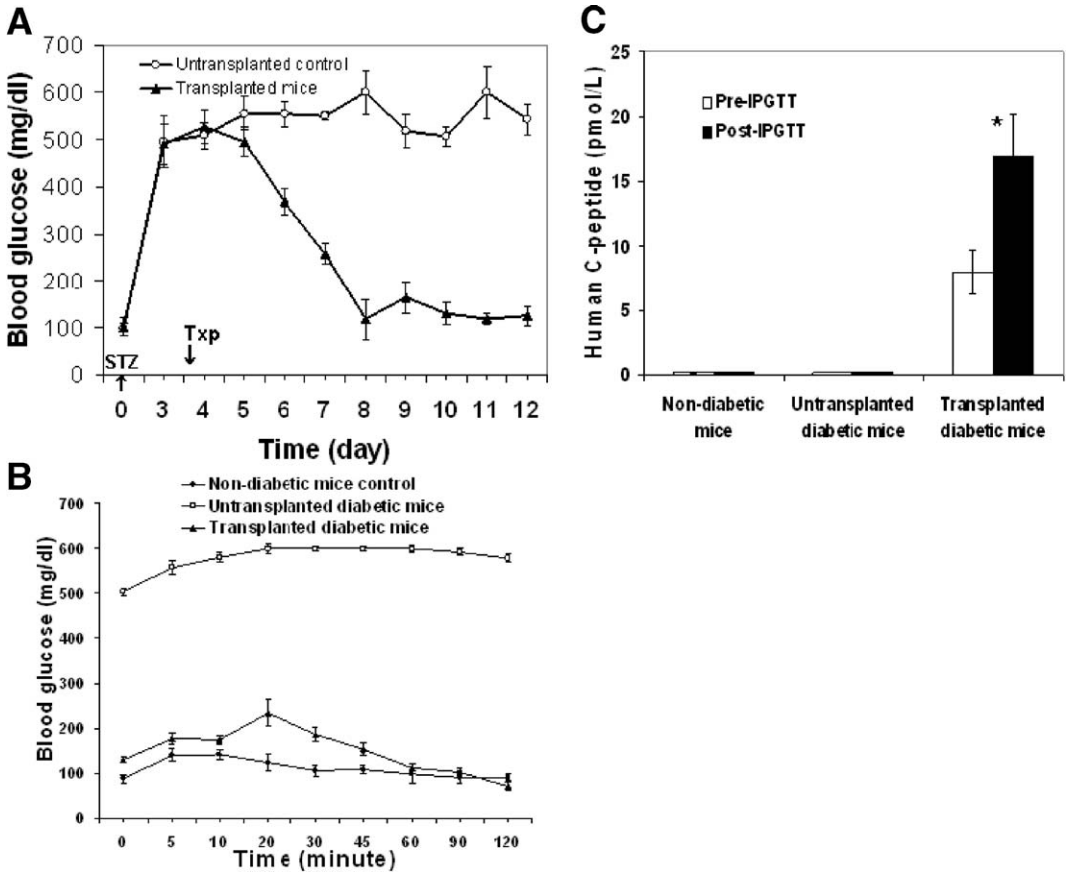


**Fig. 6 – CB–SC differentiated into functional insulin-producing cells after transplantation into streptozotocin (STZ)-induced diabetic mice. (A) Kinetic examination showed decreasing of blood glucose levels post-transplantation (Txp). *n*=7 for CB–SC-transplanted mice; *n*=8 for untransplanted diabetic mice. Glucose levels were measured from whole tail vein blood using an AccuChek glucose detector. (B) Intraperitoneal glucose tolerance testing (IPGTT) after 7 days following transplantation. *n*=3 for CB–SC-transplanted mice; *n*=4 for untransplanted diabetic mice, and *n*=3 for non-diabetic mice. (C) Human C-peptide detection in the sera of transplanted mice. Blood samples were collected during 20 min before and after IPGTT. *n*=3 for each group. Human C-peptide was examined by using an ultrasensitive human C-peptide enzyme-linked immunosorbent assay (ELISA) kit. Data represent mean (±SD). Asterisk (*) represents for *P* value<0.05.**

normal range after 60 min (Fig. 6B). However, blood glucose of CB–SC-untransplanted diabetic mice remained very high (>500 mg/dl) (Fig. 6B).

To substantiate that this reversal of hyperglycemia was associated with differentiation of CB–SC into insulin-producing cells, we performed the following experiments. Due to the cross-reactivity of antibodies between human and mouse insulin, we utilized an assay that is specific for human C-peptide (a by-product of insulin production) to evaluate human insulin secretion [27–29] from differentiated CB–SC cells. The results showed that human C-peptide was undetectable in mouse sera of CB–SC-untransplanted diabetic mice and normal non-diabetic mice, both prior to IPGTT and following IPGTT. In contrast, the human C-peptide level was significantly increased after IPGTT, to a level that was about 2 times higher than before IPGTT in the sera of the CB–SC-transplanted diabetic mice ($P<0.05$) (Fig. 6C). These experiments demonstrated that CB–SC differentiated into functional insulin-producing cells in diabetic mice.

## Discussion

Embryonic stem (ES) cells display two unique properties: self-renewal and pluripotentiality for differentiation [1]. Stem-cell-based therapy, therefore, has significant potential to cure important, and common, human diseases [2,3]. However, a major limitation for stem-cell-based therapy has been identification of a suitable source of stem cells. For instances, there are significant ethical issues for use of ES cells [6,7] and adult stem cells display reduced proliferation and differentiation ability [3]. In this report, we identify novel stem cells (CB–SC) from human umbilical cord blood. Our studies demonstrate that CB–SC expressed ES-cell-specific markers, such as the transcription factors Oct-4 and Nanog, and the stage-specific embryonic antigens SSEA-3 and SSEA-4. CB–SC can also give rise to cells with characteristics of three embryonic layers: e.g., mesoderm (endothelial-like cells), ectoderm (neuronal-like cells) and endoderm (insulin-producing cells). CB–SC therefore would be a valuable source for stem-cell-based therapeutics.

We generated CB–SC using a very basic cell culture medium with a low percentage of serum (7% FBS), without cell feeders. This is in contrast to ES cells which require cell feeders and growth factors, raising potential contamination problems [30]. Importantly, we found that CB–SC grew well and could be passaged in glass chamber slides and/or Petri dishes. Interestingly, we found that tissue culture dishes (treated by Vacuum Gas Plasma) did not support the growth of CB–SC. In comparison with ES cells, CB–SC had a more limited potential for long-term proliferation, which decreased after 3 months in culture. We speculate that further optimization of growth conditions may improve their potential for longer-term proliferation. The widespread availability of human cord blood, however, underlines the potential usefulness of CB–SC for clinical therapeutics.

Umbilical cord blood has provided an important source of stem cells for research as it has unique advantages compared to other sources of stem cells: no ethical concerns, no risk to the donors and low risk of graft-versus-host disease (GVHD) [10–12]. McGuckin et al. isolated SSEA-3$^+$, SSEA-4$^+$ and Oct-4$^+$ ES-cell-like cells from a non-hematopoietic cell population (CD45$^-$) of cord blood [18]. Compared with CB–SC, these cells grew in clumps and did not spread out in microflasks. Importantly, the rarity of this cell in cord blood (about 0.21% of mononuclear cells [18]) poses a key limitation for therapeutic usefulness. Different from other reported cord-blood-derived stem cells [14–16,31–35], CB–SC display the following characteristics: retention of hematopoietic cell antigen CD45 in long-term culture, expression of both ES cell and hematopoietic cell markers, but negative for hematopoietic stem cell marker CD34. Additionally, both immunocytochemistry and flow analysis demonstrated that CB–SC are negative for CD34 and macrophage marker CD11b/Mac-1, which is significantly different from our previously reported cord blood monocyte-derived stem cells, f-macrophage [17].

The most important property we demonstrate for CB–SC is their ability to produce a therapeutic glycemic effect in an STZ mouse model of diabetes. Diabetes and its long-term complications are increasing in prevalence, posing an important therapeutic challenge for individual patients and public health. Deficit of insulin-producing cells is the crucial issue for both type 1 and type 2 diabetic patients. In spite of the development and application of various insulin formulations, exogenous insulin neither achieves the same degree of glycemic control as that provided by endogenous insulin nor completely prevents the long-term complications such as diabetic retinopathy, neuropathy, nephropathy and diverse cardiovascular disorders [2]. These clinical challenges necessitate the development of more efficient treatments. Islet cell transplantation, a potential treatment, has been limited by a shortage of pancreas as a source of purified islets. Stem-cell-derived insulin-producing cells, therefore, provide a promising approach for beta cell-replacement therapy [2]. Accumulating evidence suggests that insulin-producing cells derived from stem cells can normalize blood glucose in diabetic animal models [2]. However, in previous reports, these cells were derived from ES cells and fetal tissues [36–41], raising ethical concerns for their clinical application. CB–SC can correct hyperglycemia in diabetic mice and restore euglycemia after an acute glucose challenge (IPGTT). We also examined production of human C-peptide (as an indicator of human insulin secretion) in the sera of CB–SC-transplanted diabetic mice. Human C-peptide production was undetectable in the sera of non-diabetic mice and untransplanted diabetic mice, but acutely increased in transplanted mice following glucose challenge. These results, in aggregate, provide evidence that CB–SC give rise to functional insulin-producing cells after transplantation into diabetic mice. This conclusion is supported by a recent report, which showed that cord blood may contain progenitors that generate insulin-producing cells [42].

In summary, using simple technology, we have generated a novel type of stem cell (CB–SC) from umbilical cord blood, displaying both embryonic and hematopoietic characteristics. Our results demonstrate that CB–SC have a high potential for expansion and differentiation and a low level of immunogenicity. Additional studies are required to further characterize the therapeutic potential of CB–SC for human disease.

## Acknowledgments

We are grateful to Shirley Bond and Yong Wang for technical assistance.

## REFERENCES

[1] A. Vats, R.C. Bielby, N.S. Tolley, R. Nerem, J.M. Polak, Stem cells, Lancet 366 (2005) 592–602.
[2] M.A. Hussain, N.D. Theise, Stem-cell therapy for diabetes mellitus, Lancet 364 (2004) 203–205.
[3] C.M. Rice, N.J. Scolding, Adult stem cells—Reprogramming neurological repair? Lancet 364 (2004) 193–199.
[4] L.M. Hoffman, M.K. Carpenter, Characterization and culture of human embryonic stem cells, Nat. Biotechnol. 23 (2005) 699–708.
[5] K.H. Wilan, C.T. Scott, S. Herrera, Chasing a cellular fountain of youth, Nat. Biotechnol. 23 (2005) 807–815.
[6] C. Dennis, E. Check, Ethical routes to stem cells highlight political divide, Nature 437 (2005) 1076–1077.
[7] M. Evans, Ethical sourcing of human embryonic stem cells–rational solutions? Nat. Rev., Mol. Cell Biol. 6 (2005) 663–667.
[8] D.A. Melton, G.Q. Daley, C.G. Jennings, Altered nuclear transfer in stem-cell research—A flawed proposal, N. Engl. J. Med. 351 (2004) 2791–2792.
[9] J. Bonde, D.A. Hess, J.A. Nolta, Recent advances in hematopoietic stem cell biology, Curr. Opin. Hematol. 11 (2004) 392–398.
[10] K.K. Ballen, New trends in umbilical cord blood transplantation, Blood 105 (2005) 3786–3792.
[11] P.R. Sanberg, A.E. Willing, S. Garbuzova-Davis, S. Saporta, G. Liu, C.D. Sanberg, P.C. Bickford, S.K. Klasko, N. El-Badri, Umbilical cord blood-derived stem cells and brain repair, Ann. N. Y. Acad. Sci. 1049 (2005) 67–83.
[12] D.A. Peterson, Umbilical cord blood cells and brain stroke injury: bringing in fresh blood to address an old problem, J. Clin. Invest. 114 (2004) 312–314.
[13] V. Silani, L. Cova, M. Corbo, A. Ciammola, E. Polli, Stem-cell therapy for amyotrophic lateral sclerosis, Lancet 364 (2004) 200–202.
[14] K. Bieback, S. Kern, H. Kluter, H. Eichler, Critical parameters for the isolation of mesenchymal stem cells from umbilical cord blood, Stem Cells 22 (2004) 625–634.
[15] E.J. Gang, S.H. Hong, J.A. Jeong, S.H. Hwang, S.W. Kim, I.H.

Yang, C. Ahn, H. Han, H. Kim, In vitro mesengenic potential of human umbilical cord blood-derived mesenchymal stem cells, Biochem. Biophys. Res. Commun. 321 (2004) 102–108.
[16] G. Kogler, S. Sensken, J.A. Airey, T. Trapp, M. Muschen, N. Feldhahn, S. Liedtke, R.V. Sorg, J. Fischer, C. Rosenbaum, S. Greschat, A. Knipper, J. Bender, O. Degistirici, J. Gao, A.I. Caplan, E.J. Colletti, G. Almeida-Porada, H.W. Muller, E. Zanjani, P. Wernet, A new human somatic stem cell from placental cord blood with intrinsic pluripotent differentiation potential, J. Exp. Med. 200 (2004) 123–135.
[17] Y. Zhao, T. Mazzone, Human umbilical cord blood-derived f-macrophages retain pluripotentiality after thrombopoietin expansion, Exp. Cell Res. 310 (2005) 311–318.
[18] C.P. McGuckin, N. Forraz, M.O. Baradez, S. Navran, J. Zhao, R. Urban, R. Tilton, L. Denner, Production of stem cells with embryonic characteristics from human umbilical cord blood, Cell Prolif. 38 (2005) 245–255.
[19] H.J. Rippon, A.E. Bishop, Embryonic stem cells, Cell Prolif. 37 (2004) 23–34.
[20] I. Klimanskaya, Y. Chung, L. Meisner, J. Johnson, M.D. West, R. Lanza, Human embryonic stem cells derived without feeder cells, Lancet 365 (2005) 1636–1641.
[21] S.H. Orkin, Chipping away at the embryonic stem cell network, Cell 122 (2005) 828–830.
[22] Y. Zhao, D. Glesne, E. Huberman, A human peripheral blood monocyte-derived subset acts as pluripotent stem cells, Proc. Natl. Acad. Sci. U. S. A. 100 (2003) 2426–2431.
[23] G. Drukker, A. Katz, M. Urbach, G. Schuldiner, J. Markel, B. Itskovitz-Eldor, O. Reubinoff, N. Mandelboim Benvenisty, Characterization of the expression of MHC proteins in human embryonic stem cells, Proc. Natl. Acad. Sci. U. S. A. 99 (2002) 9864–9869.
[24] M. Baron, Induction of embryonic hematopoietic and endothelial stem/progenitor cells by hedgehog-mediated signals, Differentiation 68 (2001) 175–185.
[25] L. Bally-Cuif, M. Hammerschmidt, Induction and patterning of neuronal development, and its connection to cell cycle control, Curr. Opin. Neurobiol. 13 (2003) 16–25.
[26] C. Andressen, S. Arnhold, M. Puschmann, W. Bloch, J. Hescheler, R. Fassler, K. Addicks, Beta1 integrin deficiency impairs migration and differentiation of mouse embryonic stem cell derived neurons, Neurosci. Lett. 251 (1998) 165–168.
[27] Y. Hori, X. Gu, X. Xie, S.K. Kim, Differentiation of insulin-producing cells from human neural progenitor cells, PLoS Med. 2 (2005) 347–356.
[28] A. Hayek, G.M. Beattie, Experimental transplantation of human fetal and adult pancreatic islets, J. Clin. Endocrinol. Metab. 82 (1997) 2471–2475.
[29] M. Zalzman, S. Gupta, R.K. Giri, I. Berkovich, B.S. Sappal, O. Karnieli, M.A. Zern, N. Fleischer, S. Efrat, Reversal of hyperglycemia in mice by using human expandable insulin-producing cells differentiated from fetal liver progenitor cells, Proc. Natl. Acad. Sci. U. S. A. 100 (2003) 7253–7258.
[30] M. Richards, C.Y. Fong, W.K. Chan, P.C. Wong, A. Bongso, Human feeders support prolonged undifferentiated growth of human inner cell masses and embryonic stem cells, Nat. Biotechnol. 20 (2002) 933–936.
[31] M. Aoki, M. Yasutake, T. Murohara, Derivation of functional endothelial progenitor cells from human umbilical cord blood mononuclear cells isolated by a novel cell filtration device, Stem Cells 22 (2004) 994–1002.
[32] D.A. Ingram, L.E. Mead, H. Tanaka, V. Meade, A. Fenoglio, K. Mortell, K. Pollok, M.J. Ferkowicz, D. Gilley, M.C. Yoder, Identification of a novel hierarchy of endothelial progenitor cells using human peripheral and umbilical cord blood, Blood 104 (2004) 2752–2760.
[33] N. Baal, K. Reisinger, H. Jahr, R.M. Bohle, O. Liang, K. Munstedt, C.V. Rao, K.T. Preissner, M.T. Zygmunt, Expression of transcription factor Oct-4 and other embryonic genes in CD133 positive cells from human umbilical cord blood, Thromb. Haemost. 92 (2004) 767–775.
[34] M. Yu, Z. Xiao, L. Shen, L. Li, Mid-trimester fetal blood-derived adherent cells share characteristics similar to mesenchymal stem cells but full-term umbilical cord blood does not, Br. J. Haematol. 124 (2004) 666–675.
[35] F.M. Cicuttini, K. Welch, A.W. Boyd, Characterization of $CD34^{+}HLA\text{-}DR^{-}$ $CD38^{+}$ and $CD34^{+}HLA\text{-}DR^{-}CD38^{-}$ progenitor cells from human umbilical cord blood, Growth Factors 10 (1994) 127–134.
[36] G.K. Brolen, N. Heins, J. Edsbagge, H. Semb, Signals from the embryonic mouse pancreas induce differentiation of human embryonic stem cells into insulin-producing beta-cell-like cells, Diabetes 54 (2005) 2867–2874.
[37] Y. Hori, I.C. Rulifson, B.C. Tsai, J.J. Heit, J.D. Cahoy, S.K. Kim, Growth inhibitors promote differentiation of insulin-producing tissue from embryonic stem cells, Proc. Natl. Acad. Sci. U. S. A. 99 (2002) 16105–16110.
[38] H. Segev, B. Fishman, A. Ziskind, M. Shulman, J. Itskovitz-Eldor, Differentiation of human embryonic stem cells into insulin-producing clusters, Stem Cells 22 (2004) 265–274.
[39] S. Miyazaki, E. Yamato, J. Miyazaki, Regulated expression of pdx-1 promotes in vitro differentiation of insulin-producing cells from embryonic stem cells, Diabetes 53 (2004) 1030–1037.
[40] M. Zalzman, L. Anker-Kitai, S. Efrat, Differentiation of human liver-derived, insulin-producing cells toward the beta-cell phenotype, Diabetes 54 (2005) 2568–2575.
[41] M. Zalzman, S. Gupta, R.K. Giri, I. Berkovich, B.S. Sappal, O. Karnieli, M.A. Zern, N. Fleischer, S. Efrat, Reversal of hyperglycemia in mice by using human expandable insulin-producing cells differentiated from fetal liver progenitor cells, Proc. Natl. Acad. Sci. U. S. A. 100 (2003) 7253–7258.
[42] S. Yoshida, F. Ishikawa, N. Kawano, K. Shimoda, S. Nagafuchi, S. Shimoda, M. Yasukawa, T. Kanemaru, H. Ishibashi, L.D. Shultz, M. Harada, Human cord blood-derived cells generate insulin-producing cells in vivo, Stem Cells 23 (2005) 1409–1416.